Date of publication MAR-31, 2024, date of current version FEB-07, 2024.
www.computingonline.net / computing@computingonline.net

Print ISSN 1727-6209
Online ISSN 2312-5381
DOI 10.47839/ijc.23.1.3433

Spatial Selection-Based Intelligent N-OFDM Signal Processing in Wireless Communication Systems

VADYM SLUSAR[1], ANDRII ZINCHENKO[2], YURIY DANYK[2], MYKHAILO KLYMASH[3], YULIIA PYRIH[3]

[1]Central Research Institute of Arms and Military Equipment of the Armed Forces of Ukraine, Kyiv 03049, Ukraine
[2]National Defense University of Ukraine named after Ivan Chernyakhovsky, Kyiv 03049, Ukraine
[3]Lviv Polytechnic National University, Lviv 79013, Ukraine

Corresponding author: Mykhailo Klymash (e-mail: mykhailo.m.klymash@lpnu.ua)

ABSTRACT The method of joint processing of pulses and OFDM (N-OFDM) signals is proposed. The corresponding analytical relations for the lower Cramer-Rao boundary on the dispersion of OFDM (N-OFDM) signals amplitude ratings in the presence of sources of pulsed radiation are obtained. Using mathematical modeling properties and limitations of the demodulation method of OFDM (N-OFDM) signals in the background of impulse signals in the integrated radar and telecommunication systems are established. It is determined that the use of the angular distance between the pulsed and OFDM signals sources at a value that is not less than 0.75 widths of the secondary beam of the digital antenna array pattern does not affect the accuracy of the OFDM signal amplitudes. The same applies to the active interferences.

KEYWORDS digital antenna array; lower bound of Cramer-Rao; block matrix; directional chart; OFDM (N-OFDM) signals.

I. INTRODUCTION

OVER recent years, digital beamforming technology has been widely developed in communication and radar sectors, software reconfiguration of equipment and MIMO (multiple input – multiple outputs). In this case, similar and sometimes identical circuit design solutions are used. This approach prompted a number of prominent scientists to promote the idea of the creation of Integrated Radar-Telecommunication Systems or Redcom Systems [1-9]. Such an idea corresponds to the Altshuler and Petrov's law of transition of the system to the super system [10-12]. This law implies that each system integrates with another system after some time, thus creating a new, enriched with additional properties over-the-system. Famous technologies for the creation of Redcom systems are widely described in scientific literature [1-9].

The most progressive view on the integration of communication systems was proposed in work [1], where it was proved that traditional methods of radar had exhausted themselves and the transition to integrated radar and telecommunication systems based on the technology of the digital antenna arrays (DAAs) and MIMO in combination with OFDM signals was justified. However, in 2010, it was proposed to create a multi-position communication and radar system using OFDM and N-OFDM signals. To implement the proposed system, several appropriate methods of digital signal processing in such systems were developed [13-21]. They were based on the time division for tasks of communication and radar-telecommunication system. Another common approach is also possible; it uses OFDM (N-OFDM) signals both in solving radar tasks and in data transmission, including using the principle of MIMO. The influence of the Doppler effect on the location of high-speed targets makes the use of OFDM technology quite problematic. The further development is a joint application of OFDM (N-OFDM) for communication and pulse signals for radar needs. However, the development of appropriate algorithmic support, which would allow simultaneous demodulation of both types of signals, as well as clarification of the conditions for its application, requires additional theoretical studies.

The purpose of the paper is to develop a method for the joint processing of pulses and OFDM (N-OFDM) signals in radar-telecommunication systems based on their spatial selection and to investigate the potential accuracy of the

proposed method.

II. MATERIALS AND METHODS

First of all, it is necessary to analyze the effect of the radio-pulse rectangular waveform on the OFDM (N-OFDM) signal response at the outputs of the frequency filters synthesized by the Fast Fourier Transform (*FFT*) operation. If the length of the rectangular radio pulse is marked as τ_i, and its power – P_i, then the energy of such a signal will be calculated according to a known expression (1):

$$E_i = P_i\tau_i = \frac{A_i^2\tau_i}{2}, \quad (1)$$

where A_i – amplitude of a rectangular radio pulse.

As a result of the *FFT* procedure over a *FFT* signal sample, the T_{FFT} energy of the said pulse is evenly distributed in the specified time interval. The effect of the radio pulse on the *FFT* response as a barrier will be equivalent to the presence of the same *FFT* pulse signal T_{FFT} with less pulse amplitude A_{iFFT}. To calculate the value of the amplitude A_{iFFT} of the equivalent pulse signal, it is necessary to solve this unknown system from two equations (2):

$$\begin{cases} E_i = P_i\tau_i = \frac{A_i^2\tau_i}{2}; \\ E_i = P_{iFFT}T_{FFT} = \frac{A_{iFFT}^2T_{FFT}}{2}. \end{cases} \quad (2)$$

From here we obtain the relation for the estimation of capacities and amplitudes as (3):

$$\begin{cases} P_{iFFT}T_{FFT} = P_i\tau_i; \\ \frac{A_{iFFT}^2T_{FFT}}{2} = \frac{A_i^2\tau_i}{2}, \end{cases} \quad (3)$$

or permanently (4):

$$\begin{cases} P_{iFFT} = P_i\frac{\tau_i}{T_{FFT}}; \\ A_{iFFT} = A_i\sqrt{\frac{\tau_i}{T_{FFT}}}. \end{cases} \quad (4)$$

In this case, the "stretching" of the pulse due to the *FFT* operation leads to an inverse proportional decrease in the power of the pulse signal and a decrease in its amplitude in $\sqrt{\tau_i/T_{FFT}}$ times. For example, if the radio pulse has a duration of 100 ns, and the length of the OFDM packet (N-OFDM) is 1 ms, that is 10,000 times bigger, then the decrease in the amplitude of the equivalent pulse after the *FFT*, consistent with the duration of the OFDM packet (N-OFDM), will be 100 times.

Based on this result, let us calculate the possible interfering level from the impact of the pulse signal on the response OFDM (N-OFDM) packet after the *FFT*. It should be noted that for the high probability of detecting the air targets reflected pulse signals, it is necessary to have some excess amplitude of the total OFDM (N-OFDM) signal pulse amplitude. Let us denote this excess of the letter *L*. The so-called peak factor of the multi-frequency OFDM (N-OFDM) signal, which is the ratio of maximum power to average power at a given interval, must be taken into account too. The presence of peak emissions in OFDM (N-OFDM) signal can cause masking of the radio pulses reflected from the target. If the peak factor is *D* times, then, in terms of amplitudes, the corresponding peak emission will exceed the mean square waveform of the signal packet in $\sqrt{D}$ times.

In order to avoid masking of the impulse signals, their amplitude must exceed in $L\sqrt{D}$ the average level of the N-OFDM packet at the input of the *FFT* operation. This means that for the above example, the overlay of a 100 nanosecond pulse and the N-OFDM millisecond packet level of equivalent impedance after *FFT* decreases to 0,01 $L\sqrt{D}$ times relative to the root mean square level of the N-OFDM before the *FFT* operation. In the case, where L = 8, and D = 64, we will receive 0,01 $L\sqrt{D}$ =0,64. Such a level of pulse noise can be induced to the forced reduction of the QAM-modulation order when transmitting an N-OFDM packet. Therefore, a more effective method for the separation of pulsed and N-OFDM signals, based on their spatial selection with the help of the DAA, deserves an attention.

Let us consider a linear DAA with an equidistant placement of antenna elements in it. It should be noted that in this case, the task of allocating pulsed signals from their mixture with continuous signals, which are conditionally OFDM (N-OFDM) signals, should be solved step by step. In the first stage, for example, the angular coordinates of the signal sources must be obtained in connection mode. For this purpose, radar guidance methods can be used, including multi-signal over-differentiation algorithms. The received information about the directions of arrival of signals allows the proceeding to the next stage of their processing, that is, estimating the general amplitudes of each type of signals. For this purpose, it is advisable to use the proposed procedure in [22]; that is why we introduce the vector of the voltage signals of the spatial receiving channels of the DAAs at separate moments of time at the outputs of the digital diagramming module in the form (5):

$$U = QW + n, \quad (5)$$

where $Q = [Q_S \mid Q_P]$- block matrix of the values of the directional patterns of the secondary spatial channels of the DAA in the directions to the OFDM (N-OFDM) (block Q_S) and pulse signal reflector (block Q_P) signals sources;

$W^T = [W_S \mid W_P]$ is the block-vector of generalized amplitudes of N-OFDM signals (block W_S) and amplitudes of pulse signals (block W_P); *"T"* is the symbol of the matrix transposition operation, *n* is the noise voltage vector.

In the general case, in the presence of *M* sources of OFDM (N-OFDM) signals and *P* pulse reflectors, the blocks of the matrix *Q* of the DAAs for *R* of the secondary spatial channels of the DAAs can be written as:

$$Q_S = \begin{bmatrix} Q_1(x_{1S}) & Q_1(x_{2S}) & \cdots & Q_1(x_{MS}) \\ Q_2(x_{1S}) & Q_2(x_{2S}) & \cdots & Q_2(x_{MS}) \\ \vdots & \vdots & \vdots & \vdots \\ Q_R(x_{1S}) & Q_R(x_{2S}) & \cdots & Q_R(x_{MS}) \end{bmatrix}, \quad (6)$$

$$Q_P = \begin{bmatrix} Q_1(x_{1P}) & Q_1(x_{2P}) & \cdots & Q_1(x_{PP}) \\ Q_2(x_{1P}) & Q_2(x_{2P}) & \cdots & Q_2(x_{PP}) \\ \vdots & \vdots & \vdots & \vdots \\ Q_R(x_{1P}) & Q_R(x_{2P}) & \cdots & Q_R(x_{PP}) \end{bmatrix}, \quad (7)$$

where $Q_r(x_m) = \left[\sin\left(\frac{R}{2}[r - x_m]\right)\right]\left[\sin\frac{1}{2}(r - x_m)\right]^{-1}$ is the orientation diagram of the *r*-th secondary spatial channel synthesized by the Fast Fourier Transform (FFT) operation; $x_{mS(pP)} = \frac{2\pi}{\lambda} d\left(r - \frac{R-1}{2}\right)\sin\theta_{mS(pP)}$ – generalized angular coordinate of *m(p)* -sources of signals relative to the normal to the DAAs; λ - the wavelength of the central carrier signals N-OFDM and pulse signals; d – a distance between antenna elements of the DAAs; R – the number of elements in the antenna array; $\theta_{mS(pP)}$ – angular coordinates of *m* (*p*) – sources of signals relative to the normal of the DAAs.

For the selection of OFDM (N-OFDM) signals in the background of the reflected pulse of the air targets, in the formation of an optimal estimation of the generalized amplitudes $\widetilde{W} = \left(Q^T Q\right)^{-1} Q^T U$ vector, a segment of the vector $\widetilde{W}$ corresponding to the OFDM (N-OFDM), block W_S, is calculated separately.

Similarly, for the selection of pulsed signals in the OFDM (N-OFDM) background, the pulse signal amplitude segment is calculated – block W_P. Further, based on the estimates of the generalized OFDM amplitudes (N-OFDM) and pulsed signals received in the series of timings, FFT procedures are performed, which allows us to synthesize the frequency filters necessary for the spectral selection of subcarriers of OFDM (N-OFDM) signals and measure the radial velocity of air targets [22].

The difference between these methods of treatment is the different principles of forming FFT filters depending on the type of signals. In particular, for the selection of subcarriers OFDM (N-OFDM), signals FFTs should be carried out on the basis of a reference unit estimates W_S, which are formed sequentially in time, at intervals of their follow-up. For pulse signals, FFT is performed over the arrays of reference blocks W_P of the estimates taken for each of the range gates through the period of repetition of pulsed signals. For OFDM (N-OFDM) signals, the FFT procedure is performed once for a character interval, and for pulse signals – *T* times, where *T* – the number of gates in the range within the interval of its unambiguous measurement. Correspondingly, the dimension of the FFT procedures may be different: for pulsed signals, it is determined by the number of *Z*-sensing periods within which airspace is monitored, whereas, for OFDM (N-OFDM) signals, the maximum length of the signal sample for FFTs can reach the values $T \times Z$.

Subsequently, the OFDM (N-OFDM) signals are demodulated by the received output voltages synthesized frequency filters, and the estimates of the trajectory parameters of the air traffic movement are calculated.

In the case of active interference, the angular coordinates of the noise generators must also be pre-evaluated and further this information is used during the demodulation of the signals optimized by the least squares method. The appropriate method of noise protection is proposed, for example, in [23]. To solve the selection problem against the background of the information OFDM (N-OFDM) and pulse signals active noise, it needs to be generalized.

The structure of the matrix Q and the vector W in the Equation (5) at the inputs of the same time receiving channels of the linear DAAs of the set of active interference, pulse and OFDM (N-OFDM) signals will accept the triblock type:

$$Q = [Q_S \mid Q_P \mid Q_J];\ W^T = [W_S \mid W_P \mid W_J], \quad (8)$$

where the elements of the block:

$$Q_J = \begin{bmatrix} Q_1(x_{1J}) & Q_1(x_{2J}) & \cdots & Q_1(x_{JJ}) \\ Q_2(x_{1J}) & Q_2(x_{2J}) & \cdots & Q_2(x_{JJ}) \\ \vdots & \vdots & \vdots & \vdots \\ Q_R(x_{1J}) & Q_R(x_{2J}) & \cdots & Q_R(x_{JJ}) \end{bmatrix}$$ are the values of the directional patterns of the secondary spatial channels of the DAAs in the direction of the j-source of noise; $x_{jJ} = \frac{2\pi}{\lambda} d\left(r - \frac{R-1}{2}\right)\sin\theta_{jJ}$ – generalized angular coordinate of the j source of noise relative to the normal of the DAAs; W_J – block of signal amplitudes of noi se.

To separate useful signals and interference, forming the optimal estimation vector amplitudes $\widetilde{W}$, only segments of this vector corresponding signals OFDM (N-OFDM) and pulse signals are calculated, that is mean W_S an W_P blocks. In this case, the segment of the vector of estimates of the amplitudes of interference signals (block W_J) is not formed at all.

In general, the statements in the case of the plane equidistant DAAs, which have a directional diagram of the

secondary spatial channels, are factorized in the form of a product of the directional diagram in two angular planes.

In the case of the structure of the DAAs with R × K elements, in this case, the Equation (5) can be rewritten using the block of Hatri-Rao matrix product:

$$U = \left[Q \left[\blacksquare \right] V \right] W + n, \qquad (9)$$

where $\left[\blacksquare \right]$ is the symbol of the Hatri-Rao block product; V is a block matrix of the values of the directional patterns of the secondary spatial channels of the DAAs in a second angular plane.

In the case of active interference, similarly (8), the structure of the matrix V in (9) will be three-block:

$$V = \left[V_S \mid V_P \mid V_J \right], \qquad (10)$$

where $V_S = \begin{bmatrix} V_1(y_{1S}) & V_1(y_{2S}) & \cdots & V_1(y_{MS}) \\ V_2(y_{1S}) & V_2(y_{2S}) & \cdots & V_2(y_{MS}) \\ \vdots & \vdots & \vdots & \vdots \\ V_K(y_{1S}) & V_K(y_{2S}) & \cdots & V_K(y_{MS}) \end{bmatrix},$

$$V_P = \begin{bmatrix} V_1(y_{1P}) & V_1(y_{2P}) & \cdots & V_1(y_{PP}) \\ V_2(y_{1P}) & V_2(y_{2P}) & \cdots & V_2(y_{PP}) \\ \vdots & \vdots & \vdots & \vdots \\ V_K(y_{1P}) & V_K(y_{2P}) & \cdots & V_K(y_{PP}) \end{bmatrix},$$

$$V_J = \begin{bmatrix} V_1(y_{1J}) & V_1(y_{2J}) & \cdots & V_1(y_{JJ}) \\ V_2(y_{1J}) & V_2(y_{2J}) & \cdots & V_2(y_{JJ}) \\ \vdots & \vdots & \vdots & \vdots \\ V_K(y_{1J}) & V_K(y_{2J}) & \cdots & V_K(y_{JJ}) \end{bmatrix},$$

$$V_r(y_m) = \left[\sin\left(\frac{Z}{2}[r - y_m] \right) \right] \left[\sin\frac{1}{2}(r - y_m) \right]^{-1},$$

$$y_{mS(pP)} = \frac{2\pi}{\lambda} d_y \left(r - \frac{R-1}{2} \right) \sin\theta_{mS(pP)} \sin\varepsilon_{mS(pP)}, \varepsilon_{mS(pP)}$$

– angular coordinates of $m(p)$ -sources of signals, relative to the normal of the DAAs in the second angular plane; d_y – the distance between the antenna elements of the DAAs in the corresponding angular plane.

In addition, a generalized angular coordinate $x_{mS(pP)} = \frac{2\pi}{\lambda} d_x \left(r - \frac{R-1}{2} \right) \sin\theta_{mS(pP)} \cos\varepsilon_{mS(pP)}$ should be used as the argument of the directional diagram matrix Q.

The considered mathematical device allows forming mathematical models of responses of receiving linear and plane DAAs in radar-telecommunication systems in the case of receiving reflected pulse signals from air targets and OFDM (N-OFDM) signals that provide data transfer functions. The obtained relations can be generalized in the case of multi-position signal processing, which is similar to works [22, 23], which makes it necessary to complicate the block structure of the corresponding matrices and to introduce additional indexes in their elements.

For example, if the set of signal voltages at the outputs of the receiving channels of the multi-sectional DAA (5) is related to the known expression:

$$U = P \cdot A + n, \qquad (11)$$

where U – block-vector of the complex voltage signals at the outputs of the spatial channels of a set of positions of the DAA multi-position system; P – signal matrix; A – block-vector amplitudes of OFDM (N-OFDM) signals and noise; n – block vector of noise stresses, then the structure of the signal matrix P and the block vectors U and A in case of the linear structure of the DAAs will be as follows:

$$P = Q \circ \tilde{H}_Q, \qquad (12)$$

where

$$Q = [Q_S \mid Q_J] = \left[\begin{array}{ccc|ccc} Q_{11}(x_{l_S}) & \cdots & Q_{11}(x_{M_S}) & Q_{11}(x_{l_J}) & \cdots & Q_{11}(x_{M_J}) \\ \vdots & \ddots & \vdots & \vdots & \ddots & \vdots \\ Q_{R1}(x_{l_S}) & \cdots & Q_{R1}(x_{M_S}) & Q_{R1}(x_{l_J}) & \cdots & Q_{R1}(x_{M_J}) \\ \hline \vdots & & \vdots & \vdots & & \vdots \\ Q_{1T}(x_{l_S}) & \cdots & Q_{1T}(x_{M_S}) & Q_{1T}(x_{l_J}) & \cdots & Q_{1T}(x_{M_J}) \\ \vdots & \ddots & \vdots & \vdots & \ddots & \vdots \\ Q_{RT}(x_{l_S}) & \cdots & Q_{RT}(x_{M_S}) & Q_{RT}(x_{l_J}) & \cdots & Q_{RT}(x_{M_J}) \end{array}\right]$$

– block matrix of the directional patterns of the antenna elements of the linear antenna array of the t-th position n $Q_{rt}\left(x_{m_{S(J)}}\right)$ in the direction towards the $m_{S(J)}$ source of OFDM (N-OFDM) signals (index S) or noise (index J) with angular coordinates $x_{m_{S(J)}}$; $r = 1, ..., R$ is the serial number of the antenna element in the lattice antennas within the t-th position; $t = 1, ..., T$ – serial position number in the multi-position system of the DAA; "T" is the symbol of the transposition operation; ∘ – the symbol of the Hadamard product;

$$\tilde{H}_Q = \left[\tilde{H}_{QS} \mid \tilde{H}_{QJ}\right] = \left[\begin{array}{ccc|ccc} \tilde{h}_{Q11_S} & \cdots & \tilde{h}_{Q11M_S} & \tilde{h}_{Q11_J} & \cdots & \tilde{h}_{Q11M_J} \\ \vdots & \ddots & \vdots & \vdots & \ddots & \vdots \\ \tilde{h}_{QR11_S} & \cdots & \tilde{h}_{QR1M_S} & \tilde{h}_{QR11_J} & \cdots & \tilde{h}_{QR1M_J} \\ \hline & \vdots & & & \vdots & \\ \tilde{h}_{Q1T1_S} & \cdots & \tilde{h}_{Q1TM_S} & \tilde{h}_{Q1T1_J} & \cdots & \tilde{h}_{Q1TM_J} \\ \vdots & \ddots & \vdots & \vdots & \ddots & \vdots \\ \tilde{h}_{QRT1_S} & \cdots & \tilde{h}_{QRTM_S} & \tilde{h}_{QRT1_J} & \cdots & \tilde{h}_{QRTM_J} \end{array}\right]$$

– block-matrix of transmission characteristics of the MIMO channel $\tilde{h}_{Qrtm_{S(J)}}$ in the direction towards the $m_{S(J)}$ source of OFDM signals (index S) or interference (index J) with angular coordinate $x_{m_{S(J)}}$; $A^T = \left[A_S \mid A_J\right]$ – block-vector amplitudes OFDM signals (block A_S) and interference (block A_J).

Based on such models, the proposed method of digital signal processing allows the division of pulsed and N-OFDM signals into the receiving system to provide a further measurement of trajectory parameters of air traffic movement and demodulation of information messages.

Subsequent studies were aimed at exploring the potential

of the proposed signal processing methods that would provide a separate selection of communication signals and radar signals in radar and telecommunication MIMO systems while simultaneously solving communication and radar problems. To estimate the level of potential errors in measuring the amplitudes of received signals, the lower bound of Cramer-Rao (CRLB) was used to disperse the measurement errors of quadrature component amplitudes of received signals formed by reversing the Fisher's information matrix. In all the above relationships, the information matrix for estimating the variances of the signal amplitude components can be written in a known form (13):

$$\mathrm{I} = \frac{1}{\sigma^2_{\text{noise}}} \cdot \mathrm{P}^{*}\mathrm{P}, \qquad (13)$$

where P is the signal matrix; σ^2 is the noise dispersion due to the Gaussian distribution.

In order to obtain CRLB for estimating the parameters of pulsed and OFDM (N-OFDM) signals simultaneously arriving at the linear receiving DAAs, during their separate spatial selection in radar and telecommunication systems we consider the case when the angular coordinates of the signal sources are precisely known. In this case, for splitting pulse selection and OFDM (N-OFDM) signals, it is necessary to evaluate the generalized amplitudes of each type of signals by (8).

Then the expression for the CRLB regarding the dispersion estimates of the vector of the generalized amplitudes W can be written down in the form described by (14) :

$$\sigma^2_W \geq \sigma^2_n diag\left[\left[Q_S \vdots Q_P \vdots Q_J\right]^T \left[Q_S \vdots Q_P \vdots Q_J\right]\right]^{-1}, \qquad (14)$$

where σ^2_n is the noise dispersion in a separate time reference signal of the signal mix at the output of the second spatial channel in the linear DAA; $diag[Z]$ – a vector formed from the diagonal elements of the matrix Z .

When transferring the (14) to the noise dispersion at the output of an analog-to-digital converter (ADC), the effect of increasing the noise dispersion should be taken into account when performing FFT according to the expression:

$$\sigma^2_n = R\sigma^2_{ADC}, \qquad (15)$$

where R - the dimension of spatial fast Fourier transform (FFT), in this case this is the number of elements of the DAA; σ^2_{ADC} - noise dispersion at the output of the ADC.

Therefore, (14) can be rewritten as:

$$\sigma^2_W \geq \sigma^2_{ADC} \cdot R \cdot diag\left[\left[Q_S \vdots Q_P \vdots Q_J\right]^T \left[Q_S \vdots Q_P \vdots Q_J\right]\right]^{-1}. \qquad (16)$$

In the case of using a flat, equidistant DAA of $R \times K$ elements, which has directional diagrams of secondary spatial channels, factorized in the form of the product of the directivity patterns in two angular planes, is needed go from (8) to (9).

This expression for CRLB can be written as:

$$\sigma^2_W \geq \sigma^2_n diag\left[\left(Q\ [\blacksquare]\ V\right)^T \left(Q\ [\blacksquare]\ V\right)\right]^{-1}, \qquad (17)$$

or

$$\sigma^2_W \geq \sigma^2_n diag\left[\begin{array}{l}\left(\left[Q_S \vdots Q_P \vdots Q_J\right]\ [\blacksquare]\ \left[V_S \vdots V_P \vdots V_J\right]\right)^T \\ \cdot\left(\left[Q_S \vdots Q_P \vdots Q_J\right]\ [\blacksquare]\ \left[V_S \vdots V_P \vdots V_J\right]\right)\end{array}\right]^{-1}. \qquad (18)$$

Taking into account the well-known identities:

$$\left[\mathrm{A}\ [\blacksquare]\ \mathrm{B}\right]^{\mathrm{T}} = \mathrm{A}^{\mathrm{T}}[\square]\,\mathrm{B}^{\mathrm{T}}, \qquad (19)$$

$$\left(\left[\mathrm{A}_{\mathrm{ji}}\right][\square]\left[\mathrm{B}_{\mathrm{ji}}\right]\right)\left(\left[\mathrm{K}_{\mathrm{ik}}\right][\blacksquare]\left[\mathrm{M}_{\mathrm{ik}}\right]\right) = \left[P_{jk} = \sum_i \left\{\left(\mathrm{A}_{\mathrm{ji}} \cdot \mathrm{K}_{\mathrm{ik}}\right) \circ \left(\mathrm{B}_{\mathrm{ji}} \cdot \mathrm{M}_{\mathrm{ik}}\right)\right\}\right], \qquad (20)$$

where $[\square]$ the symbol of the block end product of block matrixes , (17) can be rewritten as follows:

$$\sigma^2_W \geq \sigma^2_n diag\left[\left(Q^{\mathrm{T}}[\square]\ V^T\right)\left(Q\ [\blacksquare]\ V\right)\right]^{-1} = \sigma^2_n diag\left[\begin{array}{l}\left(\left[\begin{array}{c}Q_S^T \\ Q_P^T \\ Q_J^T\end{array}\right][\square]\left[\begin{array}{c}V_S^T \\ V_P^T \\ V_J^T\end{array}\right]\right) \\ \cdot\left(\left[Q_S \vdots Q_P \vdots Q_J\right]\ [\blacksquare]\ \left[V_S \vdots V_P \vdots V_J\right]\right)\end{array}\right]^{-1} \qquad (21)$$

or

$$\sigma^2_W \geq \sigma^2_n diag\left[\left[\begin{array}{c}Q_S^T\left[Q_S \vdots Q_P \vdots Q_J\right] \\ Q_P^T\left[Q_S \vdots Q_P \vdots Q_J\right] \\ Q_J^T\left[Q_S \vdots Q_P \vdots Q_J\right]\end{array}\right] \circ \left[\begin{array}{c}V_S^T\left[V_S \vdots V_P \vdots V_J\right] \\ V_P^T\left[V_S \vdots V_P \vdots V_J\right] \\ V_J^T\left[V_S \vdots V_P \vdots V_J\right]\end{array}\right]\right]^{-1} =$$

$$= \sigma^2_n diag\left[\begin{array}{l}\left[\begin{array}{ccc}Q_S^T Q_S & Q_S^T Q_P & Q_S^T Q_J \\ Q_P^T Q_S & Q_P^T Q_P & Q_P^T Q_J \\ Q_J^T Q_S & Q_J^T Q_P & Q_J^T Q_J\end{array}\right] \circ \\ \circ\left[\begin{array}{ccc}V_S^T V_S & V_S^T V_P & V_S^T V_J \\ V_P^T V_S & V_P^T V_P & V_P^T V_J \\ V_J^T V_S & V_J^T V_P & V_J^T V_J\end{array}\right]\end{array}\right]^{-1} =$$

$$= \sigma^2_n diag\left[\begin{array}{ccc}Q_S^T Q_S \circ V_S^T V_S & Q_S^T Q_P \circ V_S^T V_P & Q_S^T Q_J \circ V_S^T V_J \\ Q_P^T Q_S \circ V_P^T V_S & Q_P^T Q_P \circ V_P^T V_P & Q_P^T Q_J \circ V_P^T V_J \\ Q_J^T Q_S \circ V_J^T V_S & Q_J^T Q_P \circ V_J^T V_P & Q_J^T Q_J \circ V_J^T V_J\end{array}\right]^{-1}. \qquad (22)$$

Recalculation of the noise at the output of the ADC is carried out in accordance with the expression: $\sigma^2_n = R \cdot K \cdot \sigma^2_{ADC}$, where R and K - the dimensions of the spatial fast Fourier transform (FFT) at two angular

coordinates.

In particular, for (22) we obtain:

$$\sigma_W^2 \geq RK\sigma_{ADC}^2 \cdot \cdot diag\left[\begin{array}{c|c|c} Q_S^T Q_S \circ V_S^T V_S & Q_S^T Q_P \circ V_S^T V_P & Q_S^T Q_J \circ V_S^T V_J \\ \hline Q_P^T Q_S \circ V_P^T V_S & Q_P^T Q_P \circ V_P^T V_P & Q_P^T Q_J \circ V_P^T V_J \\ \hline Q_J^T Q_S \circ V_J^T V_S & Q_J^T Q_P \circ V_J^T V_P & Q_J^T Q_J \circ V_J^T V_J \end{array}\right]^{-1}. \quad (23)$$

In the absence of interference, (23) is simplified as:

$$\sigma_W^2 \geq RK\sigma_{ADC}^2 diag\left[\begin{array}{c|c} Q_S^T Q_S \circ V_S^T V_S & Q_S^T Q_P \circ V_S^T V_P \\ \hline Q_P^T Q_S \circ V_P^T V_S & Q_P^T Q_P \circ V_P^T V_P \end{array}\right]^{-1}. \quad (24)$$

The presence of interferences leads to an increase in the size of the Fisher information matrix, which causes an increase in the dispersion magnitude, that is, the effect of interferences and worse accuracy in evaluating generalized signal amplitudes.

Inequalities (23), (24) characterize the lower bound of dispersions for estimates of quadrature components of generalized signal amplitudes obtained by (25, 26):

$$\mathrm{W}^{\mathrm{c}} = \mathrm{Re}\left(\left\{ \left(Q\ [\blacksquare]\ V\right)^T \left(Q\ [\blacksquare]\ V\right) \right\}^{-1} \left(Q\ [\blacksquare]\ V\right)^T \mathrm{U} \right), \quad (25)$$

$$\mathrm{W}^{\mathrm{S}} = \mathrm{Im}\left(\left\{ \left(Q\ [\blacksquare]\ V\right)^T \left(Q\ [\blacksquare]\ V\right) \right\}^{-1} \left(Q\ [\blacksquare]\ V\right)^T \mathrm{U} \right), \quad (26)$$

where:

$$\mathrm{W}^{\mathrm{c}} = \left[\mathrm{W}_{1\mathrm{S}}^{\mathrm{c}} \quad \mathrm{W}_{2\mathrm{S}}^{\mathrm{c}} \quad \cdots \quad \mathrm{W}_{\mathrm{MS}}^{\mathrm{c}} \mid \mathrm{W}_{1\mathrm{P}}^{\mathrm{c}} \quad \mathrm{W}_{2\mathrm{P}}^{\mathrm{c}} \quad \cdots \quad \mathrm{W}_{\mathrm{PP}}^{\mathrm{c}} \mid \mathrm{W}_{1\mathrm{J}}^{\mathrm{c}} \quad \mathrm{W}_{2\mathrm{J}}^{\mathrm{c}} \quad \cdots \quad \mathrm{W}_{\mathrm{JJ}}^{\mathrm{c}}\right]^{\mathrm{T}},$$

$$\mathrm{W}^{\mathrm{S}} = \left[\mathrm{W}_{1\mathrm{S}}^{\mathrm{s}} \quad \mathrm{W}_{2\mathrm{S}}^{\mathrm{s}} \quad \cdots \quad \mathrm{W}_{\mathrm{MS}}^{\mathrm{s}} \mid \mathrm{W}_{1\mathrm{P}}^{\mathrm{s}} \quad \mathrm{W}_{2\mathrm{P}}^{\mathrm{s}} \quad \cdots \quad \mathrm{W}_{\mathrm{PP}}^{\mathrm{s}} \mid \mathrm{W}_{1\mathrm{J}}^{\mathrm{s}} \quad \mathrm{W}_{2\mathrm{J}}^{\mathrm{s}} \quad \cdots \quad \mathrm{W}_{\mathrm{JJ}}^{\mathrm{s}}\right]^{\mathrm{T}}.$$

The obtained dispersion estimates can then serve as noise dispersions in calculating the accuracy of impulse and OFDM (N-OFDM) signal estimation at the subsequent stages of their digital processing, in particular, in the case of performing a fast Fourier transform (FFT) over a series of sequentially formed in time subvectors of generalized amplitude estimates of OFDM (N-OFDM) signals. $\mathrm{W}_{\mathrm{Sn}} = \mathrm{W}_{\mathrm{Sn}}^{\mathrm{C}} + j\mathrm{W}_{\mathrm{Sn}}^{\mathrm{S}} = \left[\mathrm{W}_{1\mathrm{Sn}}^{\mathrm{c}} \quad \mathrm{W}_{2\mathrm{Sn}}^{\mathrm{c}} \quad \cdots \quad \mathrm{W}_{\mathrm{MSn}}^{\mathrm{c}}\right]^{\mathrm{T}} + j\left[\mathrm{W}_{1\mathrm{Sn}}^{\mathrm{s}} \quad \mathrm{W}_{2\mathrm{Sn}}^{\mathrm{s}} \quad \cdots \quad \mathrm{W}_{\mathrm{MSn}}^{\mathrm{s}}\right]^{\mathrm{T}}$ expression for CRLB variances of estimates of N-OFDM signal amplitudes with the same frequency grid for all directions in receiving has the form:

$$\sigma_A^2 \geq \sigma_{\mathrm{w}}^2 \otimes \left(N \cdot diag\left[F^T F\right]^{-1}\right), \quad (27)$$

or

$$\sigma_A^2 \geq RK\sigma_{ADC}^2 diag\left[\begin{array}{c|c|c} Q_S^T Q_S \circ V_S^T V_S & Q_S^T Q_P \circ V_S^T V_P & Q_S^T Q_J \circ V_S^T V_J \\ \hline Q_P^T Q_S \circ V_P^T V_S & Q_P^T Q_P \circ V_P^T V_P & Q_P^T Q_J \circ V_P^T V_J \\ \hline Q_J^T Q_S \circ V_J^T V_S & Q_J^T Q_P \circ V_J^T V_P & Q_J^T Q_J \circ V_J^T V_J \end{array}\right]^{-1} \otimes \left(N \cdot diag\left[F^T F\right]^{-1}\right), \quad (28)$$

- in the presence of active interference and

$$\sigma_W^2 \geq RK\sigma_{ADC}^2 diag\left[\begin{array}{c|c} Q_S^T Q_S \circ V_S^T V_S & Q_S^T Q_P \circ V_S^T V_P \\ \hline Q_P^T Q_S \circ V_P^T V_S & Q_P^T Q_P \circ V_P^T V_P \end{array}\right]^{-1} \otimes \left(N \cdot diag\left[F^T F\right]^{-1}\right), \quad (29)$$

- in the absence of interference, where $\mathrm{F} = \begin{bmatrix} \dot{F}_1(\omega_1) & \cdots & \dot{F}_1(\omega_T) \\ \vdots & \cdots & \vdots \\ \dot{F}_N(\omega_1) & \cdots & \dot{F}_N(\omega_T) \end{bmatrix}$ – the matrix of amplitude-frequency characteristics (AFCs) $\dot{F}_n(\omega_t)$, synthesized by means of FFT operation of N frequency filters at T carrier frequencies of N-OFDM signals, $\otimes$ – a symbol of the Kronecker product of matrixes.

The dispersion estimates of pulse signal parameters, in particular, Doppler frequency shift, time of arrival, can be calculated similarly.

In the course of further research, the properties of the obtained analytical relations are determined by mathematical modeling in the Mathcad package and the limits of the OFDM (N-OFDM) demodulation signals are set against the background of the action of the pulse signals of selecting the air targets. At the same time, for the sake of simplification of calculations, the assumption has been made that there is no active interference.

In the course of mathematical modeling, the mean square deviation (SDM) of the amplitudes estimates is determined in the ADC quanta. In this case, the ADC bit size does not matter, because, for any bit, the size of the ADC quantum value must be aligned with the root mean square noise (for example, they must be equal in magnitude).

The angular diversity of signal Δ sources is set in the fractions of the chart main petal of the DAA direction. At the same time, in order to reduce the amount of computations

during the research, the step of changing the angle distribution of the signal sources is set equal to 0.1 width of the main petal directional diagram in the range of angular distances from 1 to 0.1 width of the directional diagram secondary beam and 0.01 – in the range from 0,1 to 0.01 beam width.

Figures 1-6 show the results of mathematical modeling of the process of estimating the quadrature component amplitudes of the OFDM signal in a separate reference frame of the DAA on the background of the pulsed radiation source with a different angular distance between it and the source OFDM (horizontal axis). The values of the quadrature amplitude components obtained with the value of the Squares are deferred vertically. The number of antenna elements in the DAA for the indicated illustrations is 4, 16 and 64. In addition to the obtained values of the square deviation mean (SDM) of the amplitudes estimates in the figures, the estimated value of the CRLB and the limits of its confidence interval for the reliability of 0.95 are given.

The obtained results confirm the well-known scientific position that when increasing the number of antenna elements of the DAA in R times of the CRLB values of the SDM, the amplitudes are reduced in the fold in $\sqrt{R}$ times.

Most precisely this regularity works for orthogonal angular spacing, that is, the width of the secondary ray, but its manifestation is noticeable with smaller differences in the angular coordinates.

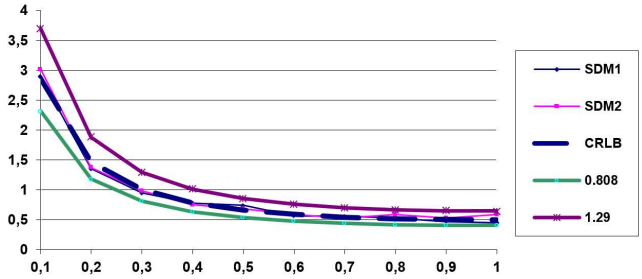

Figure 1. Dependence of the SDM error estimating amplitudes of signals from angular diversity of signal sources (4-element DAA).

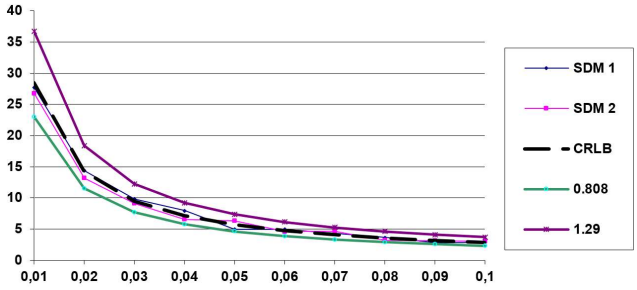

Figure 2. Dependence of the SDM error estimating amplitudes of signals from angular diversity of signal sources (4-element DAA).

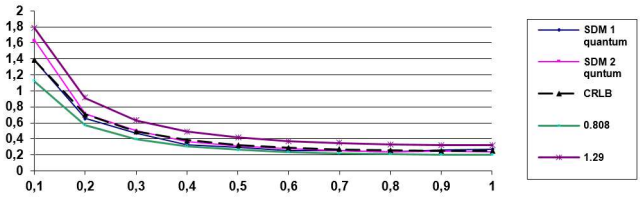

Figure 3. Dependence of the SDM error estimating amplitudes of signals from angular diversity of signal sources (16-element DAA).

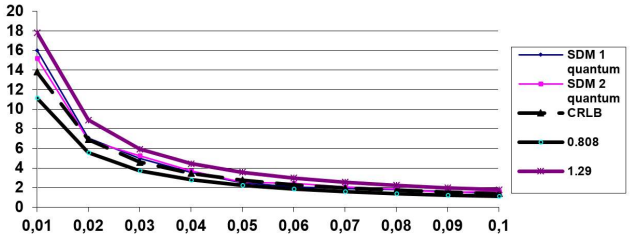

Figure 4. Dependence of the SDM error estimating amplitudes of signals from angular diversity of signal sources (16-element DAA).

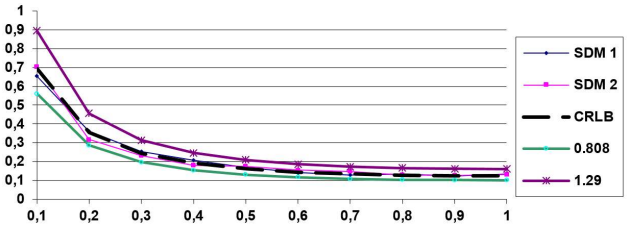

Figure 5. Dependence of the SDM error estimating amplitudes of signals from angular diversity of signal sources (64-element DAA).

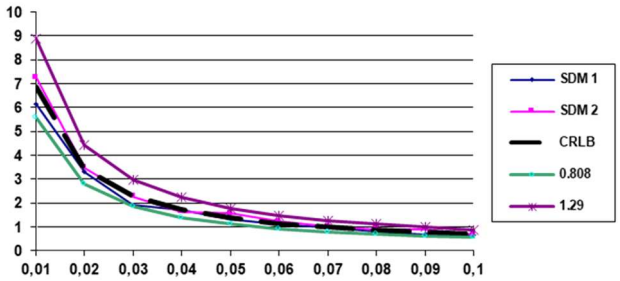

Figure 6. Dependence of the SDM error estimating amplitudes of signals from angular diversity of signal sources (64-element DAA).

For example, at angular separation of signal sources at 0.1 widths of the upper limit directional diagram, the secondary beam of the confidence interval is about 1.8 quantum ADC for a 16-elements DAA and 0.9 for a 64-elements DAA, and an increase in the number of antenna elements is by 4 times to a two-fold decrease in the magnitude of the SDM estimates of amplitude.

However, for the first time, for the two-stage evaluation of signal parameters, it is established, that regardless of the number of antenna elements in the DAA at the magnitude of the angular diversity of two sources less than 0.1 of the width of the secondary beam, directional diagram of the CRLB for

SDM estimation of quadrature component signal amplitudes decreases directly in proportion to the reduction of angular diversity.

For example, in Figure 5 and Figure 6, the upper limit of the confidence interval of the SDM (0.9 quantum ADC) at angle distributions 0.01 is 10 times less than the corresponding magnitude (9 quantum of ADC) for angular resolution 0.1. The same can be traced on the charts for the 16-elements and 4-elements DAA. In more detail, the corresponding pattern is illustrated in Table 1 for a 16-elements DAA case.

Based on the obtained results, it is possible to formulate an approximate empirical dependence for calculating the potentially possible value of the SDM estimates of quadrature components of signal amplitudes σ_a for the case of angular diversity of two sources by magnitude, less than 0.05 width of the secondary beam directional diagram of the DAA:

$$\sigma_a \approx 0{,}552\frac{\sigma_{ADC}}{\Delta\sqrt{R}}, \quad (30)$$

where σ_{ADC} – SDM noise at the output of the ADC in the fractions of the ADC quantum, Δ – an angular separation of radiation sources in fractions of the secondary beam of the DAA directional diagram, R – a number of antenna elements in the DAA.

Table 1. Results of a mathematical experiment to estimate quadrature component of amplitudes of signals from two sources of radiation for a 16-elements DAA

Angle distributions	**0,01**	**0,02**	**0,03**	**0,04**	**0,05**
SDM Re-part	16,00762364063	7,08273378525	4,96604507259	3,55101217215	2,48308680676
SDM Im-part	15,21118998969	6,82238152971	5,27592568829	3,72152332322	2,55936412585
CRLB	13,811125245	6,90691784153	4,60611803314	3,45617050588	2,76656431932
0,808 CRLB	11,15938919796	5,58078961596	3,72174337078	2,79258576875	2,23538397001
1,29 CRLB	17,81635156605	8,90992401557	5,94189226276	4,45845995259	3,56886797192
Angle distributions	**0,06**	**0,07**	**0,08**	**0,09**	**0,1**
SDM Re-part	2,06512572943	1,89773861823	1,82312482486	1,58170743279	1,3855681331
SDM Im-part	2,45087930186	2,08224513074	1,84814456956	1,51387786047	1,63548621551
CRLB	2,30712926193	1,97922104478	1,73351759985	1,54261784623	1,39008119658
0,808 CRLB	1,86416044364	1,59921060418	1,40068222068	1,24643521976	1,12318560683
1,29 CRLB	2,97619674789	2,55319514776	2,2362377038	1,98997702164	1,79320474358
Angle distributions	**0,2**	**0,3**	**0,4**	**0,5**	**0,6**
SDM Re-part	0,65633827706	0,47396662017	0,32744893379	0,29026547432	0,25658532661
SDM Im-part	0,70939775604	0,50715891436	0,36641200421	0,30901120082	0,27510699818
CRLB	0,70878204683	0,48812909244	0,38301680246	0,32453559254	0,28978868853
0,808 CRLB	0,57269589384	0,39440830669	0,30947757639	0,26222475877	0,23414926033
1,29 CRLB	0,91432884041	0,62968652924	0,49409167517	0,41865091438	0,3738274082
Angle distributions	**0,7**	**0,8**	**0,9**	**1,0**	
SDM Re-part	0,25733587778	0,23621369299	0,26534275327	0,26626281599	
SDM Im-part	0,25384552527	0,2360208778	0,24495568963	0,24150272577	
CRLB	0,26898727825	0,25719243828	0,25152254019	0,25	
0,808 CRLB	0,21734172082	0,20781149013	0,20323021248	0,202	
1,29 CRLB	0,34699358894	0,33177824539	0,32446407685	0,3225	

Directly proportional to the angular range difference in the number of antenna elements of the DAA in determining the CRLB SDM of amplitude components is possible approximately to the angular distance of 0.2 width of the beam of the DAA directional diagram.

For example, according to the results of a mathematical experiment, at a differentiation angle of 0.1 in a 64-element DAA, the CRLB SDM amplitude value (0.6937914361) is approximately equal to the value of the CRLB SDM (0.70878204683) for a 16-element DAA at an angle between sources of 0.2. That is, in the specified interval of changes of the angular distances at a fixed value of SDM amplitudes, achieving a decrease in the maximum permissible angular diversity of the signal sources by N times requires an increase in the number of antenna elements of the DAA by N^2 times.

III. CONCLUSIONS

For the purpose of simultaneous implementation of communication and radar tasks simultaneously in space and time, in the article, for the first time the method for selecting pulse signals, reflected from radar targets, in the presence of OFDM (N-OFDM) signals providing the realization of communication functions is proposed. A distinctive feature of the considered mathematical apparatus is providing mathematical models formation for receiving linear and plane digital antenna arrays of radar and telecommunication systems in the case of simultaneous receiving reflected signals from the air targets of the pulses and OFDM (N-OFDM) signals that provide data transfer functions. A mathematical experiment is carried out to show that when the angular diversity of sources of pulse and OFDM signals with a value that is not less than 0.75 width of a secondary beam of CD DAA, the presence of the second source is almost unaffected on the accuracy of the estimation of signal amplitudes. The same applies to the effects of active interference. If in the DAA, an N-bit ADC is applied, one of the digits of which is a sign, then in the specified spatial sector provided, there is no output signal of the signal mixture beyond the aperture, the ADC can potentially provide a breakdown from impulse

exposure or a noise source at the level of 6×(*N*-1) dB. For example, by a 16-bit ADC it is the limit in 6×15=90dB, which is quite sufficient for the selection of small-scale air targets by means of a pulse signal with the simultaneous reception of OFDM (N-OFDM) communication signals.

If narrow the specified corner sector, then the recovery efficiency from an additional source of signals, the indicator of which is the level of SDM estimates of amplitudes, will worsen. This necessitates the separation of the OFDM communication task into radar-based pulse signals. Analyzing, for example, the data of Table 1, it is easy to notice, that the transition from orthogonal angular diversity from Δ=1 to Δ=0,07 leads to an increase in the level of SDM approximately in 8 times (from 0.25 to 2). Thus, such a significant narrowing of the spatial diversity of the pair of signal sources leads to an increase in SDM of 18 dB amplitude ratings, that for further signal processing in a two-stage procedure should actually be considered as the corresponding increase in noise measurements of signal parameters. Additional compression of the spatial sector to Δ=0.035 adds 6 dB to the level of SDM estimates of the amplitudes that make total 24 dB, which reduces the level of disassembly continuous (OFDM) signal from pulse (intermittent). In the above case, the 16-bit ADC will lead to a potentially possible disassembly level of 90 – 24 = 66 dB, which is also quite acceptable.

It should also be noted that due to the accumulation of the OFDM signals in time in the synthesis of the frequency filters using the Fast Fourier Transform procedure of the specified values, that delay from the pulse (noise) signal will increase. However, in the practical implementation of the proposed approach given estimates of the achievable level of oppression mutual influence of the sources of the two signals will need to be adjusted taking into account the negative factors, that is due to the non-identity of the frequency response of the receiving channels and the antenna elements direction diagrams of the DAA, limited accuracy of information about angular coordinates of signal sources, nonlinearity of analog segment of receiving channels in conjunction with non-linearity of aperture ADC and so on. Detailed assessments of the impact of these and other negative factors go beyond the scope of this work.

Overall, the proposed approach can be suitable for the future intelligent 5G mobile networks, since the use of OFDM in combination with spatial selection is a powerful tool for improving communication quality, in particular, minimizing the effects of intersymbol interference, etc. [24-28].

References

[1] P. Quaranta, "Radar technology for 2020," *Military Technology*, vol. 48, no. 9, pp. 86–89, 2016.

[2] C. Sturm, W. Wiesbeck, "Waveform design and signal processing aspects for fusion of wireless communications and radar sensing," *Proceedings of the IEEE,* vol. 99, no. 7, pp. 1236–1269, 2011. https://doi.org/10.1109/JPROC.2011.2131110.

[3] L. C. Parode, "Ku-band integrated radar," *Communications Subsystem for the Shuttle, the Record of the IEEE 1977 Mechanical Engineering in Radar Symposium*, 1977, pp. 21-26. [Online]. Available at: http://www.dtic.mil/cgibin/GetTRDoc?AD=ADA303213#page=34.

[4] R. H. Cager, Jr., D. T. La Flame, L. C. Parode, "Orbiter Ku-band integrated radar and communications subsystem," *IEEE Trans. Commun*, vol. COM-26, no. 11, pp. 1604-1619, 1978. https://doi.org/10.1109/TCOM.1978.1094004.

[5] R. K. Sanapala and S. R. Duggirala, "A secure LEACH protocol for efficient CH selection and secure data communication in WSNs," *International Journal of Computer Network and Information Security (IJCNIS)*, vol. 14, no. 5, pp. 82-93, 2022, https://doi.org/10.5815/ijcnis.2022.05.07.

[6] D. B. Darshan and C. R. Prashanth, "Dual-discriminator conditional generative adversarial network optimized with hybrid momentum search algorithm and Giza pyramids construction algorithm for cluster-based routing in WSN assisted IoT," *International Journal of Computer Network and Information Security (IJCNIS)*, vol. 15, no. 5, pp. 96-112, 2023, https://doi.org/10.5815/ijcnis.2023.05.09.

[7] S. Hongbo, D. K. P. Tan, Y. Lu, "Design and implementation of an experimental GSM based passive radar," *Proceedings of the International Radar Conference*, 3-5 Sept. 2003, pp. 418–422.

[8] R. Zemmari, B. Knoedler, U. Nickel, "GSM passive coherent location: improving range resolution by mismatched filtering," *Proceedings of the 2013 IEEE Radar Conference (RadarCon13)*, 2013, pp. 1–6. https://doi.org/10.1109/RADAR.2013.6586014,

[9] R. Zemmari, M. Broetje, G. Battistello, U. Nickel, "GSM passive coherent location system: performance prediction and measurement evaluation," *IET Radar Sonar Navig*, vol. 8, no. 2, pp. 94–105, https://doi.org/10.1049/iet-rsn.2013.0206.

[10] G. S. Altshuller, *Creativity as an Exact Science. Theory of Inventive Problem Solving*, 1979, 184 p.

[11] G. S. Altshuller, *Find the Idea. Introduction to the Theory of Solving Inventive Problems,* 1986, 209 p.

[12] P. Kathiroli and S. Kanmani, "Localization by Salp Swarm Optimization with Doppler Effect in Wireless Sensor Networks," *International Journal of Computer Network and Information Security (IJCNIS)*, vol. 13, no. 6, pp. 26-40, 2021, https://doi.org/10.5815/ijcnis.2021.06.03.

[13] T. Maksymyuk, L. Han, X. Ge, H. Chen and M. Jo, "Quasi-quadrature modulation method for power-efficient video transmission over LTE networks," *IEEE Transactions on Vehicular Technology*, vol. 63, no. 5, pp. 2083-2092, 2014, https://doi.org/10.1109/TVT.2014.2313658.

[14] G. Spica Sujeetha, "A multi-objective fuzzy logic based multi-path routing algorithm for WSNs," *International Journal of Wireless and Microwave Technologies (IJWMT)*, vol. 12, no. 1, pp. 30-40, 2022, https://doi.org/10.5815/ijwmt.2022.01.04.

[15] M. Klymash et al., "Spectral efficiency increasing of cognitive radio networks," *Proceedings of the 2013 12th International Conference on the Experience of Designing and Application of CAD Systems in Microelectronics (CADSM)*, Polyana Svalyava, 2013, pp. 169-171.

[16] R. Vatambeti, V. K. Damera, H. Karthikeyan, M. Manohar, C. Sharon Roji Priya, and M. S. Mekala, "Classification of HHO-based machine learning techniques for clone attack detection in WSN," *International Journal of Computer Network and Information Security (IJCNIS),* vol. 15, no. 6, pp. 1-15, 2023, https://doi.org/10.5815/ijcnis.2023.06.01.

[17] H. Kim, I. Jung, Y. Park, W. Chung, S. Choi and D. Hong, "Time spread-windowed OFDM for spectral efficiency improvement," *IEEE Wireless Communications Letters*, vol. 7, no. 5, pp. 696-699, 2018, https://doi.org/10.1109/LWC.2018.2812150.

[18] M. Sadek and S. Aissa, "Leakage based precoding for multi-user MIMO-OFDM systems," *IEEE Transactions on Wireless Communications*, vol. 10, no. 8, pp. 2428-2433, 2011, https://doi.org/10.1109/TWC.2011.062111.101748.

[19] T. Maksymyuk and V. Pelishok, "The LTE channel transmission rate increasing," *Proceedings of International Conference on Modern Problem of Radio Engineering, Telecommunications and Computer Science*, Lviv-Slavske, 2012, pp. 251-252.

[20] B. Zheng, F. Chen, M. Wen, F. Ji, H. Yu and Y. Liu, "Low-complexity ML detector and performance analysis for OFDM with In-Phase/Quadrature index modulation," *IEEE Communications Letters*, vol. 19, no. 11, pp. 1893-1896, 2015, https://doi.org/10.1109/LCOMM.2015.2474863.

[21] P. Aggarwal and V. A. Bohara, "A nonlinear downlink multiuser MIMO-OFDM systems," *IEEE Wireless Communications Letters*, vol.

6, no. 3, pp. 414-417, 2017, https://doi.org/10.1109/LWC.2017.2699195.

[22] V. Slyusar, "A two-stage digital processing of NOFDM signals received from multiple UAV in planar digital antenna array," *Proceedings of the 4th International Scientific Conference on Defensive Technologies OTEH,* Belgrade, Serbia, 6-7 October, 2011, pp. 408-410.

[23] V. I. Slyusar , M. O. Masesov, "The method of space-time coding of tropospheric communication signals on the basis of the improved technology of multi-MIMO," *Collection of Scientific Works of VITI NTUU "KPI",* 2009, pp. 132-136.

[24] P. A. Guskov et al., "Methods and techniques of spectrum refarming for LTE network deployment," *Proceedings of the 2013 23rd International Crimean Conference "Microwave & Telecommunication Technology"*, Sevastopol, Ukraine, 2013, pp. 474-475.

[25] B. Fekade et al., "Clustering hypervisors to minimize failures in mobile cloud computing," *Wireless Communications and Mobile Computing*, vol. 16, no. 18, pp. 3455-3465, 2016. https://doi.org/10.1002/wcm.2770.

[26] F. A. P. de Figueiredo, N. F. T. Aniceto, J. Seki, I. Moerman and G. Fraidenraich, "Comparing f-OFDM and OFDM performance for MIMO systems considering a 5G scenario," *Proceedings of the 2019 IEEE 2nd 5G World Forum (5GWF)*, Dresden, Germany, 2019, pp. 532-535, https://doi.org/10.1109/5GWF.2019.8911702.

[27] H. N. Parajuli, J. Poëtte and E. Udvary, "UF-OFDM based radio over fiber for 5G millimeter wave small cell radio access network," *Proceedings of the 2018 IEEE 11th International Symposium on Communication Systems, Networks & Digital Signal Processing (CSNDSP)*, Budapest, Hungary, 2018, pp. 1-4, https://doi.org/10.1109/CSNDSP.2018.8471805.

[28] G. Barb, M. Otesteanu, F. Alexa and F. Danuti, "OFDM multi-numerology for future 5G new radio communication systems," *Proceedings of the 2020 International Conference on Software, Telecommunications and Computer Networks (SoftCOM)*, Split, Croatia, 2020, pp. 1-3, https://doi.org/10.23919/SoftCOM50211.2020.9238308.

***VADYM SLUSAR** is a Doctor of Technical Sciences, Professor majoring in Military Cybernetics, Control and Communication Systems, Honored Scientist of Ukraine. Head of the Group of Chief Scientific Staff of the Central Research Institute of Weapons and Military Equipment of the Armed Forces of Ukraine.*

Scientific interests: radar systems, smart antennas for wireless communications and digital beamforming.

***ANDRII ZINCHENKO** is a Doctor of Technical Sciences, Professor. Head of the Communication and Automated Control Systems Department of the Institute of Information Technologies, National Defense University of Ukraine named after Ivan Chernyakhovsky.*

Scientific interests: information technology, telecommunications, cybersecurity, radar.

***YURIY DANYK** is a Doctor of Technical Sciences, Professor, Honored Scientist and Technician of Ukraine, Laureate of the State Award of Ukraine in Science and Technology. Chief of the Institute of Information Technologies Ivan Chernyakhovsky National Defense University of Ukraine.*

Scientific interests: ensuring cyber security of Ukraine, information technology.

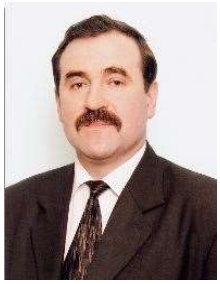

***MYKHAILO KLYMASH** is a Doctor of Technical Sciences, Professor, an academician of the Academy of Communications of Ukraine and the International Academy of Informatization, a Laureate of the State Award in Science and Technology. Head of the Telecommunications Department of the Lviv Polytechnic National University.*

Scientific interests: optical transport telecommunication networks and systems, radio networks.

***YULIIA PYRIH** is a Candidate of Technical Sciences majoring in Telecommunication Systems and Networks. Assistant of the Department of Telecommunications of the Lviv Polytechnic National University.*

Scientific interests: routing of information flows, self-organizing networks, IoT, distributed information systems.